

78. The Restoring Force Characteristics of Multi-storey Frames

By Minoru WAKABAYASHI

(Manuscript received October 13, 1964)

1. Introduction

In an aseismatic design of structures, structures were designed so as to resist the static horizontal load at each story. The accumulation of many vibration records of strong earthquakes, the advance in the non-linear vibration theories and the progress in analog and digital computers make it possible to design structures by a dynamic analysis. In the dynamic design of structures, it is necessary to represent the complex structures by some mechanical systems containing some concentrated masses connected with linear or non-linear springs. In the analysis of such systems, it is necessary to determine the relation between the horizontal load and the relative displacement at each storey, i.e., the restoring force characteristics in elastic and elasto-plastic regions. There is little theoretical results or experimental data on the restoring force characteristics of existing or experimental frames.

The author will conduct research on the following two subjects in this respect.

First, the relation between the vertical load and the restoring force is discussed here. In multi-story building frames, the axial force of a column at lower stories is large. When the frame is displaced laterally, the axial force produces the additional moment to the column. The additional moment has been ignored in designing the structures, but in the design of multi-story frames, it should not be ignored. In this paper, the effect of the axial force of the column on the elastic characteristics of multi-story frames is to be discussed theoretically. The revised theory of Muto's method¹⁾ usually adopted in static analysis, is proposed here in consideration of the effect of the axial force. Further, with the aim of investigating the relationship between the axial force of columns and the strength of structures or the restoring force characteristics after yielding, the experiment on miniature portal frames is carried out, and their elasto-plastic characteristics are discussed.

In the second place, to investigate the elasto-plastic characteristic of frames under repeated horizontal loading, the experiment of portal frames is carried out. At each cycle of loads, the absorbed energy is calculated. Their energy absorption is a very important factor in investigating the damping capacity of the elasto-plastic vibration of structures.

2. The elastic behaviour and practical method of analysis of tall frames subjected to horizontal and vertical loading

2.1. *The buckling length of columns in tall frames.*

The buckling length of columns of portal frames fixed at their base is equal

to the column length h or $2h$, corresponding to the relative stiffness ratio of beams ∞ or 0 , respectively. For ordinary relative stiffness ratio it is between h and $2h$. With the increase in the number of stories the ratio of the buckling length to h , l_{kr}/h of frames becomes larger. A certain minimum stiffness of the horizontal member, therefore, is necessary to keep the buckling length within economic limits. Fig. 1 illustrates the relation between the buckling

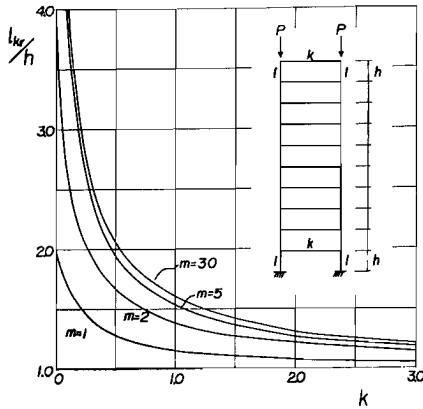


Fig. 1. Buckling length of single-bay frames, fixed at the base.

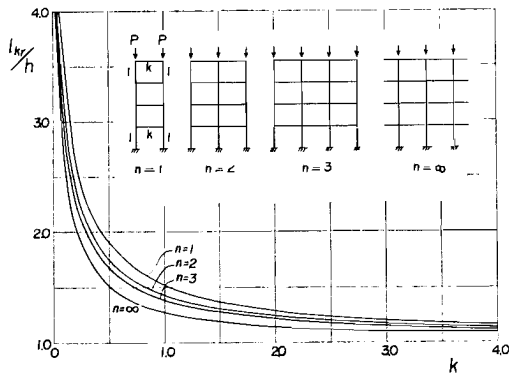


Fig. 2. Buckling length of four-story frames, fixed at the base.

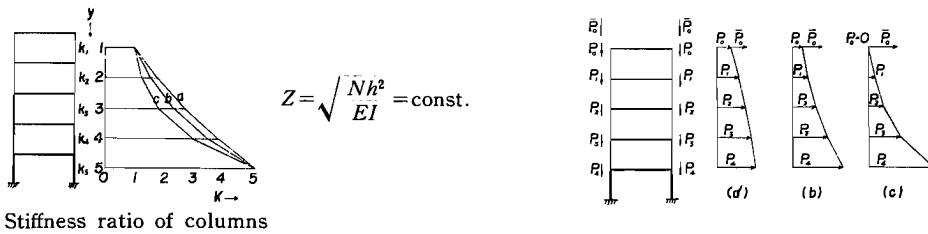
length of columns in single-bay rectangular frames divided by the column length and the relative stiffness ratio of beams for several numbers of stories. It will be noted that the ratio l_{kr}/h of 5-story frames is approximately equal to that of 30-story frames. The buckling length is affected by the number of bays. Fig. 2 shows the buckling length of 4-story frames with several bays²⁾. With the increase in the number of bays the restraint of beams against the end rotation of columns is liable to be intensified and the buckling length becomes shorter. It is found that the buckling length of frames having an infinitely large number of bays with the relative stiffness ratio of beams k_B , is equal to that of single bay frames whose relative stiffness ratio of beams is $2k_B$.

In the foregoing discussion several simplifications are made; (1) every column and beam have the same moment of inertia and length; (2) the column load is applied at the top of the column. These assumptions deviate from conditions which prevail in real building frames. More practical cases are analysed and the results are shown in Fig. 3³⁾. In these cases, in order to simplify the calculation, the column load and the moment of inertia of beams and columns vary from storey to storey following a fixed rule; all the columns would buckle at the same time, if they were pin-supported at both ends. According to the design data of the Tokyo Station building project¹⁾, this assumption is satisfactory for every storey except the top. (Table 1) Fig. 3 shows that provided the above assumption is satisfied, the buckling length does not differ from

length of columns in single-bay rectangular frames divided by the column length and the relative stiffness ratio of beams for several numbers of stories. It will be noted that the ratio l_{kr}/h of 5-story frames is approximately equal to that of 30-story frames. The buckling length is affected by the number of bays. Fig. 2 shows the buckling length of 4-story frames with several bays²⁾. With the increase in the number of bays the restraint of beams against the end rotation of columns is liable to be intensified and the buckling length becomes shorter. It is found that the

buckling length of frames having an infinitely large number of bays with the relative stiffness ratio of beams k_B , is equal to that of single bay frames whose relative stiffness ratio of beams is $2k_B$.

In the foregoing discussion several simplifications are made; (1) every column and beam have the same moment of inertia and length; (2) the column load is applied at the top of the column. These assumptions deviate from conditions which prevail in



Stiffness ratio of columns

Fig. 3. Buckling length of a five-storey frame. The axial loads and stiffness of columns vary from storey to storey.

k_b	$k = \text{const.}$		$k_5 = 5k_1$				
	(1)	(a)		(b)		(c)	
	L_k/h	L_k/h	$\frac{(a)-(1)}{(1)}$	L_k/h	$\frac{(b)-(1)}{(1)}$	L_k/h	$\frac{(c)-(1)}{(1)}$
0.5	1.9306	1.9311	+0.03	1.9187	-0.61	1.8978	-1.70
1.0	1.5372	1.5388	+1.10	1.5298	-0.49	1.5221	-0.98
1.5	1.3798	1.3792	-0.04 (%)	1.3748	-0.36 (%)	1.3682	-0.84 (%)

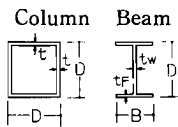
$$k_b = \frac{2 \times (\text{Beam Stiffness})}{k_{n-1} + k_n}$$

k_n = Column Stiffness of n^{th} story

TABLE 1. Project of Tokyo Station.

(cm.)

Seismic Coefficient : 0.2
Steel . JIS SM 50 ($\sigma_Y = 3,300 \text{ kg/cm}^2$)



Storey	Column		Beam			
	D	t	B	tw	D	tw
25	60	1.6	25	1.9	60	0.9
20	65	1.9	30	2.8	70	0.9
15	70	2.2	35	3.2	80	0.9
10	75	2.8	40	3.2	90	1.2
5	80	3.2	45	3.2	100	1.2
1	85	4.0	50	3.2	110	1.2
B4	95	6.0	55	3.2	120	1.2

Storey	Axial Load $N(t)$	Column Length $h(\text{cm})$	$Z^2 = \frac{Nh^2}{EI}$	Slenderness ratio
25	34.9	350.0	8.91×10^{-3}	29.19
20	193	350.0	32.69	26.90
15	363	350.0	42.49	24.95
10	543	350.0	42.53	23.72
5	734	350.0	37.93	21.78
1	942	412.5	47.28	24.08
B4	1079	500.0	35.82	25.12

Storey	Buckling Load $N_k(t)$	$N_E = \frac{\pi^2 EI}{h^2}$ (100t)	$N_y = \sigma_y A$ (t)	N/N_k (%)	N/N_{E_s} (%)	N/N_y (%)
25	1107	386.9	1121	3.15	0.09	3.11
20	1423	582.6	1439	13.53	0.33	13.41
15	1773	843.4	1790	20.47	0.43	20.28
10	2406	1261.4	2426	22.59	0.43	22.40
5	2930	1826.3	2949	25.07	0.40	24.90
1	3856	1966.9	3888	24.43	0.47	24.23
B4	6348	2973.7	6408	17.00	0.36	16.84

that in the example shown in Fig. 1.

In order to get the buckling length of real uniform building frames, therefore, it will be permissible to get the buckling length from Fig. 1 regarding the frames as single-bay frames and to correct it according to the number of bays in reference to Fig. 2.

In general the buckling length of rectangular frames is closely related to their flexural rigidity. Taking this nature into account, the author reported⁶⁾ in 1954 a method of calculating the buckling length of frames, but further investigations have not yet been made into tall frames; the effect of varying relative stiffness ratios of columns and the effect of arbitrary combinations

of column loads and moments of inertia of columns have not been studied.

2.2. The reduction of the flexibility and the additional bending moment caused by the axial load of columns.

The buckling load of rectangular frames corresponding to the buckling length of columns discussed in the previous section is, as a matter of fact, the vertical load which causes the frames a lateral deflection without horizontal loading. In real building frames the axial load of columns is not so large as the buckling load, for columns are designed safely enough against the vertical load. Table 1 expressly indicates that the ratio N/N_k (where N is the column load and N_k is the

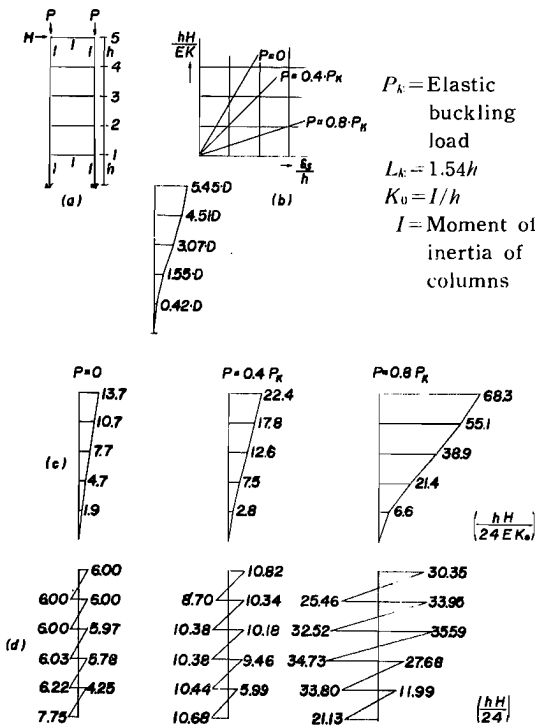


Fig. 4. Reduction of the flexural rigidity.

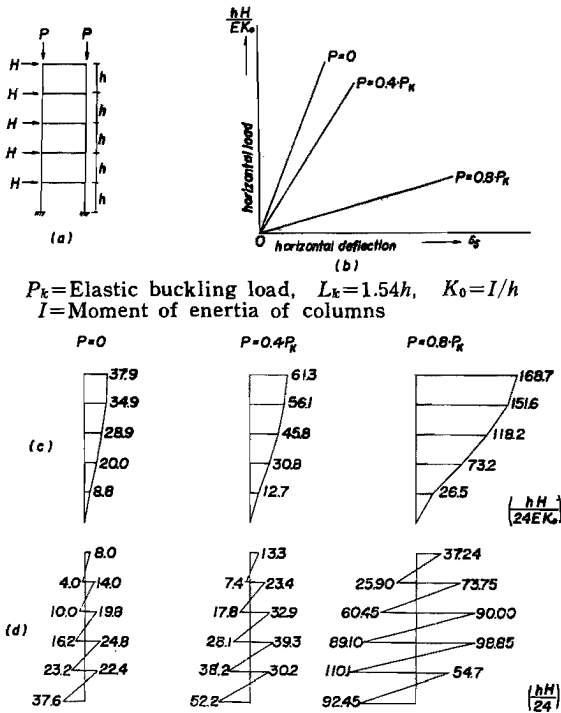


Fig. 5. Reduction of the flexibility.

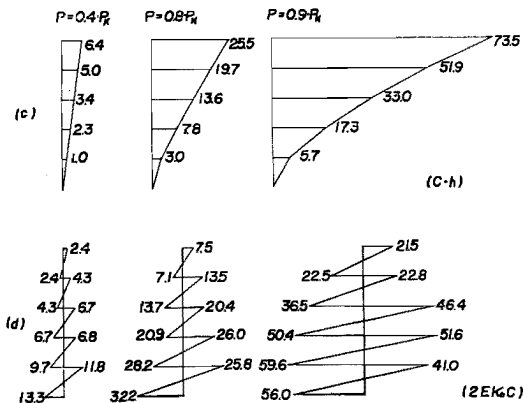
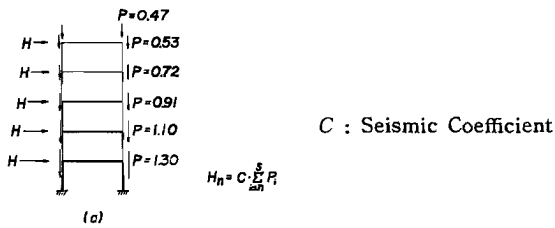


Fig. 6. Reduction of the flexibility.

buckling load of columns) is about 0.13 to 0.25. Even such a small amount of column load decreases the flexibility of columns.

The reduction of flexibility makes the fundamental period of structures longer and is considered to be favorable for aseismic analysis of structures; nevertheless, considering the additional moment mentioned below and the reduction of ductility after the bearing capacity is reached, the reduction in the flexibility may be unfavorable. Figs. 4, 5, 6 show the reduction in the flexibility for several values of the column load. In these figures, (c) and (d) show the deflection curves and the bending moment diagrams of columns, respectively. The lower end bending moment of columns subjected to shearing force Q and axial load N (Fig. 7) is the sum of the bending moment $Q\eta h$ and the additional bending moment $N\delta$, where ηh is the height of the inflection point. Figs. 4 (d), 5(d) and 6(d) show the increase in the end

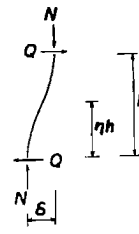


Fig. 7.

bending moment for the increasing column load.

2.3. Revision of Muto's practical aseismatic design method of structures.

Muto's practical aseismatic design method of structures consists of two processes : The first process is to decide the shearing force distribution in vertical members using D-values, the shearing force distribution coefficients ; the second is to get the inflection point and bending moment of columns. This method is based on the analysis of uniform rectangular frames, and the effect of the vertical load is disregarded here. As was discussed in the previous section, the axial load of columns of multi-storied frames decreases their flexibility and increases the bending moment in columns. We are now concerned with the analysis of rectangular frames subjected to vertical and horizontal loading in an attempt to show a method for the correction of Muto's theory.

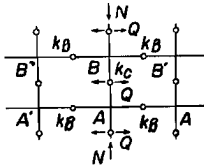


Fig. 8.

i) The shearing force distribution coefficients of columns

We now take up the problem of a continuous frame (Fig. 8), every column of which is subjected to the same shearing force and vertical load. Assuming that the inflection points of columns and beams are at the middle of each member the end bending moments of columns and beams are obtained by the slope-deflection

method as follows :

$$\left. \begin{aligned} M_{AB} = M_{BA} &= 2EK_0k_C(\gamma\theta - \gamma R) \\ M_{AA'} = M_{BB'} &= 2EK_0k_B(3\theta) \end{aligned} \right\} \quad (1)$$

where θ = angle of joint rotation
 R = slope angle of columns
 K_0 = standard stiffness ratio of members
 k_B, k_C = relative stiffness ratio of beams and columns
 E = Young's modulus
 $\gamma = \alpha + \beta$

$$\alpha = \frac{1}{2} \cdot \frac{Z \sin Z - Z^2 \cos Z}{2(1 - \cos Z) - 2Z \sin Z}$$

$$\beta = \frac{1}{2} \cdot \frac{Z^2 - Z \sin Z}{2(1 - \cos Z) - 2Z \sin Z}$$

$$Z = \sqrt{\frac{hN}{EK_0k_C}}$$

The equilibrium equations of moments at joint A and the shearing forces of columns are

$$\left. \begin{aligned} M_{AB} + M_{AA'} &= 0 \\ Q &= -\frac{2M_{AB}}{h} - NR \end{aligned} \right\} \quad (2)$$

Substituting eq. (1) into eq. (2) and solving for Q,

$$Q = \frac{\gamma \bar{k}}{2\gamma + 3\bar{k}} \cdot k_C \cdot \frac{12EK_0R}{h} - NR$$

where $\bar{k} = \frac{2k_B}{k_O}$.

Using the relations $Z = \sqrt{\frac{hN}{EK_0k_O}}$ and $\delta = Rh$, the above equation can be written in the form

$$Q = \left(\frac{\gamma \bar{k}}{2\gamma + 3\bar{k}} - \frac{Z^2}{12} \right) \cdot k_O \cdot \frac{12EK_0}{h^2} \delta. \quad (3)$$

According to the definition of the shearing force distribution coefficient D , the following relation is obtained :

$$D = \frac{Q}{\delta} = \left(\frac{\gamma \bar{k}}{2\gamma + 3\bar{k}} - \frac{Z^2}{12} \right) k_O, \quad (4)$$

the unit of D being that of $\frac{12EK_0}{h^2}$.

For ordinary frames, the relative stiffness ratio \bar{k} is obtained as follows (Fig. 9) :

$$\bar{k} = \frac{k_1 + k_2 + k_3 + k_4}{2k_O} \quad (5)$$

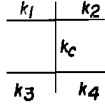


Fig. 9.

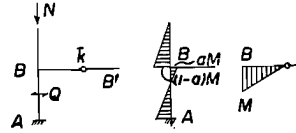


Fig. 10.

The D-value of columns fixed at one end is obtained by applying the same procedure outlined above. The end bending moments are as follows (Fig. 10) :

$$\left. \begin{aligned} M_{AB} &= 2EK_0k_O(\beta\theta_B - \gamma R) \\ M_{BA} &= 2EK_0k_O(\alpha\theta_B - \gamma R) \\ M_{BB'} &= 2EK_0k_B(3\theta_B) \end{aligned} \right\} \quad (6)$$

The equilibrium equations are

$$\left. \begin{aligned} M_{BA} &= -aM_{BB'} \\ Q &= -\frac{M_{AB} + M_{BA}}{h} - NR \end{aligned} \right\} \quad (7)$$

Solving eqs (6) and (7) for Q , we obtain

$$Q = \frac{1}{6} \left(\frac{\alpha - \beta + 6a\bar{k}}{\alpha + 3a\bar{k}} \cdot \gamma - \frac{Z^2}{2} \right) k_O \cdot \frac{12EK_0\delta}{h^2}. \quad (8)$$

Assuming $a = \frac{1}{3}$, we have

$$Q = \frac{1}{6} \left(\frac{\alpha - \beta + 2\bar{k}}{\alpha + \bar{k}} \cdot \gamma - \frac{Z^2}{2} \right) k_O \cdot \frac{12EK_0\delta}{h^2}. \quad (9)$$

According to the definition, we obtain the D-value of columns fixed at one end ;

$$D = \frac{Q}{\delta} = \frac{1}{6} \left(\frac{\alpha - \beta + 2\bar{k}}{\alpha + \bar{k}} \cdot \gamma - \frac{Z^2}{2} \right) k_O \quad (10)$$



In the case of Fig. 11, the relative stiffness ratio \bar{k} is given by

$$\bar{k} = \frac{k_1 + k_2}{k_c} \quad (11)$$

Fig. 11. ii) The standard height of the inflection point of columns

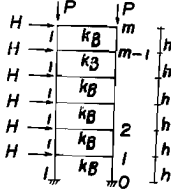


Fig. 12.

The standard height of the inflection point of columns can be derived from the analysis of uniform continuous frames. Fig. 12 shows the frame and the assumed loading. The relative stiffness ratio of beams to columns is k . In the following analysis the increment of the axial load of columns caused by the shearing force of beams being neglected; the frame in Fig. 12 shows the same behavior for continuous frames having beams whose relative stiffness ratio is $k/2$.

Applying the slope-deflection method, the end bending moment of columns and beams at joint n and the shearing force of columns of the n^{th} storey are obtained as follows;

$$\left. \begin{aligned} M_{n,n-1} &= 2EK(\alpha\theta_n + \beta\theta_{n-1} - \gamma R_n) \\ M_{n,n+1} &= 2EK(\alpha\theta_n + \beta\theta_{n+1} - \gamma R_{n+1}) \\ M_{nn} &= 2EKk(3\theta_n) \\ Q_n &= -\frac{2EK}{h}\{\gamma(\theta_n + \theta_{n-1}) - \delta R_n\} \end{aligned} \right\} \quad (12)$$

where K = stiffness ratio of columns

h = column length

θ_n = joint rotation at joint n

R_n = slope angle of n^{th} storey

$$\delta = 2\gamma - \frac{Z^2}{2}$$

$$Z = \sqrt{\frac{Ph}{EK}}$$

The moment equilibrium equation at joint n is given by

$$M_{n,n-1} + M_{nn} + M_{n,n+1} = 0 \quad (13)$$

Substituting eq. (12) into eq. (13), we get

$$\beta\theta_{n+1} + (2\alpha + 3k)\theta_n + \beta\theta_{n-1} - \gamma(R_n + R_{n+1}) = 0 \quad (14)$$

From the equilibrium of forces at n^{th} storey, we get another equation:

$$Q_n = (m - n + 1)H \quad (15)$$

Substituting eq. (12) into eq. (15), we get

$$R_n = \frac{1}{\delta} \left\{ \gamma(\theta_n + \theta_{n-1}) + \frac{hH}{2EK}(m - n + 1) \right\} \quad (16)$$

Eliminating R_n and R_{n+1} with the use of eq. (16), eq. (14) is written as follows:

$$\theta_{n+1} - 2\gamma\theta_n + \theta_{n-1} = \frac{hH}{2EK} \cdot \frac{\gamma}{\beta\delta - \gamma^2} (2m - 2n + 1) \quad (17)$$

where

$$g = -\frac{\alpha\delta - \gamma^2 + \frac{3}{2}k\delta}{\beta\delta - \gamma^2} \quad (18)$$

Eq. (17) being valid for $n=1, 2, \dots, m-1$, we have $m-1$ equations of this type. In order to determine $m+1$ joint rotations two additional equations are needed. One of these equations is obtained from the assumption that the bases are fixed;

$$\theta_0 = 0 \quad (19)$$

The other equation is obtained by applying the same procedure outlined above to the top joint m . This leads to the equation

$$(\gamma^2 - \beta\delta)\theta_{m-1} + \{\gamma^2 - \delta(3k + \alpha)\}\theta_m = -\frac{hH}{2EK}\gamma \quad (20)$$

Considering eq. (17) as a second order finite difference equation which must satisfy the boundary conditions (19) and (20), we obtain the solution as follows;

$$\theta_n = C_1 \cosh \lambda_n + C_2 \sinh \lambda_n + \frac{\gamma(2m-2n+1)}{2\gamma\delta - 4\gamma^2 + 3k\delta} \cdot \frac{hH}{2EK} \quad (21)$$

where $\lambda = \cosh^{-1} g$

$$\left. \begin{aligned} C_1 &= -\frac{\gamma}{2\gamma\delta - 4\gamma^2 + 3k\delta} \cdot (2m+1) \frac{hH}{2EK} \\ C_2 &= -\frac{\gamma[(\alpha - \beta)\delta - (2m+1)\{(\gamma^2 - \beta\delta) \cosh(m-1)\lambda + (\gamma^2 - \alpha\delta - 3k\delta) \cosh m\lambda\}]}{(2\gamma\delta - 4\gamma^2 + 3k\delta)[(\gamma^2 - \beta\delta) \sinh(m-1)\lambda + (\gamma^2 - \alpha\delta - 3k\delta) \sinh m\lambda]} \cdot \frac{hH}{2EK} \end{aligned} \right\} \quad (22)$$

The end bending moments of columns are obtained by substituting eq. (16) into eq. (12):

$$\left. \begin{aligned} M_{n-1,n} = M_n &= \left(\alpha - \frac{\gamma^2}{\delta}\right)\theta_{n-1} + \left(\beta - \frac{\gamma^2}{\delta}\right)\theta_n - \frac{\gamma}{\delta}(m-n+1)hH \\ M_{n,n-1} = M_{\bar{n}} &= \left(\beta - \frac{\gamma^2}{\delta}\right)\theta_{n-1} + \left(\alpha - \frac{\gamma^2}{\delta}\right)\theta_n - \frac{\gamma}{\delta}(m-n+1)hH \end{aligned} \right\} \quad (23)$$

Assuming the value of Z , we can determine the joint rotation θ_n from eq. (21), and then the bending moments of columns from eq. (23).

The standard height of the inflection point of columns is easily derived from Fig. 13 as

$$y_n = \frac{M_n}{M_{\bar{n}} + M_n} \quad (24)$$

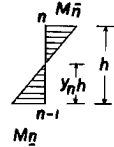


Fig. 13.

The value of y_n was calculated for several frames by the author. The results show that the effect of the axial load of columns on the standard height of inflection point is small enough to be negligible.

iii) The bending moment of columns subjected to shearing force and axial load.

If the axial load of columns is known, we can obtain the D-value of columns

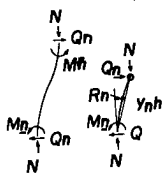


Fig. 14.

from eq. (4) or (10) and we can determine the shearing force distribution. The height of inflection point y is obtained by referring to Muto's tables.

The bending moment of columns is derived from Fig. 14 as

$$\left. \begin{aligned} M_{\bar{n}} &= Q_n y_n h + N R_n y_n h = \left(1 + \frac{Z^2 k_0}{12 D_n}\right) Q_n y_n h \\ M_{\bar{n}} &= \left(1 + \frac{Z^2 k_0}{12 D_n}\right) Q_n (1 - y_n) h \end{aligned} \right\} \quad (25)$$

where D_n and k_0 are the shearing force distribution coefficient and the relative stiffness ratio of columns, respectively.

3. Elasto-plastic behavior of frames subjected to vertical and horizontal loads

3.1. A general survey of recent researches.

In the foregoing discussion frames were treated in terms of elasticity. The slenderness ratio of columns scheduled to be used in Tokyo Station is about 20~30 (ref. Table 1); therefore the problem of frame behavior under vertical load is in the range of the plastic buckling.

Moreover plastic range is taken into account in dynamic vibrational analysis of frames subjected to the earthquake force, so that it is of great significance to recognize what will happen to the load-deflection relation in that range.

When only the horizontal load is applied to a frame, it increases until the frame attains to a mechanism, followed by the formation of adequate yield hinges at the joints of the frame and the frame becomes unstable. (ref. Fig. 15) After the formation of a mechanism a frame sustains a constant maximum horizontal load in the process of deflection. On the contrary, when a horizontal load is applied to the frame subjected to constant vertical loads, the maximum load with which the frame becomes unstable is small in comparison with the former instance, and it decreases once above the stability limit under the influence of the vertical load-deflection effect (ref. Fig. 15).

Kato has investigated the load-deflection relation of columns fixed at both

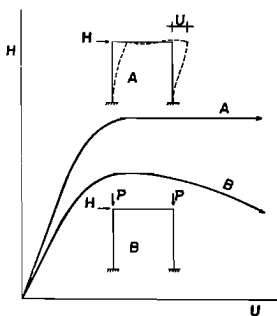


Fig. 15. Load-deflection curve.

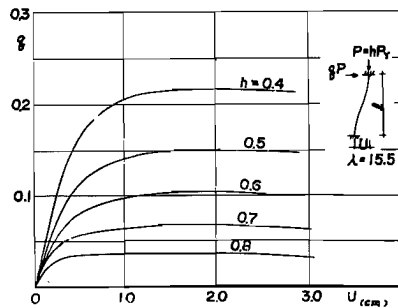


Fig. 16. Load-deflection curve.

ends subjected to the large axial force with the axial stress $0.4 \sim 0.8 \sigma_y$ (σ_y : yield stress), and to the horizontal load which is applied to the top of columns⁶⁾. The slenderness ratios are 17.5 and 31.

The calculative method is similar to Ježek's approximate method of the column strength on the assumption that the material is ideally elasto-plastic, and that the deflection curve is looked upon as a sine curve, and is solved from equilibrium condition of the internal and the external forces at their members' ends. Fig. 16 illustrates the solution by this method.

Makino has indicated a method concerned with frame behavior in the elasto-plastic range similar to Ježek's accurate method of the column strength, under equilibrium conditions of the internal and the external forces throughout the member. Fig. 17 illustrates a solution by this method.

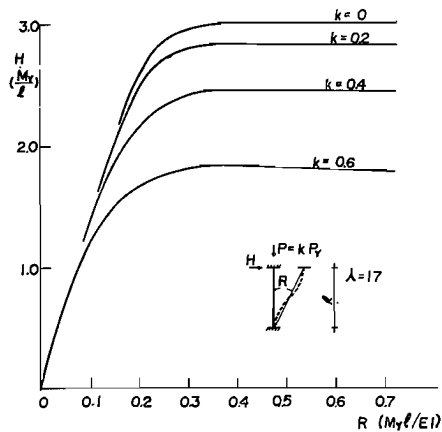


Fig. 17. Load-deflection curve.

Oxford has investigated a continuous beam over four supports with rectangular cross sections, the center span being subjected to a compressive force and a lateral load at its center, and he has made use of these results in the case of an elbow frame and has drawn a load-deflection curve⁸⁾.

Here both the vertical load P and the lateral load nN increase, and the ratio of the axial force of the column N to nN is constant, so that this load condition differs from that of the earthquake force. Vogel has studied the same frame investigated by Oxford and obtained the load-deflection curve on the assumption that in the members of the frame yield hinges are formed in due order at the cross sections where the internal moment attains to the full plastic moment and that the frame becomes a mechanism⁹⁾.

In Fig. 18 the solid line shows Oxford's result.

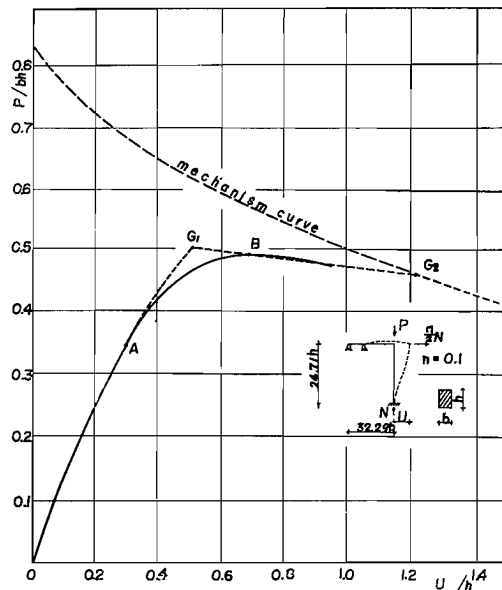


Fig. 18. Load-deflection curve.

At point A yield begins at the compression side of the cross section. At point B frame becomes unstable. The dotted line shows Vogel's

result. At point G_1 the first yield hinge is created at the bottom of the column, and at point G_2 the second one is created at its top, that is, point G_2 indicates the attainment of a mechanism.

3.2. Model tests on steel portal frames.

Experiments were conducted to investigate the effect of the axial force on the elastic-plastic behavior of tall steel buildings subjected to the earthquake, particularly on the horizontal ultimate strength, deformation capacity within the limit of stability and deformation property in the range of frame instability. Models were end fixed steel portal frames consisting of beams and columns with rectangular cross sections and were cut off by a machine from 10 mm mild steel plates without heating. Two frames were welded by 6 mm ϕ bar at joints and at the centers of the beams and columns to avoid lateral buckling before the attainment of a frame collapse mechanism in the plane of the frame. The yield stress of the materials obtained from the tension tests was 2.73 t/cm² or 2.50 t/cm².

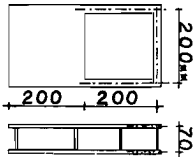


Fig. 19. Test frame.

The span and column height were both 200 mm, the same dimensions being used throughout all models. (ref. Fig. 19)

The slenderness ratios λ were 100, 50 and 30, the effective length being taken as the column height.

The beam/column stiffness ratios were 0.5 and 1.0.

Therefore the models were divided into six series. The vertical loads are 0%, 10%, 20% and 40% of the elastic ($\lambda=100$) or the plastic buckling load P_c of models ($\lambda=50, 30$). It was applied to the tops of the columns of all the models by two oil jacks, each having 10 tons capacity, and was maintained constant while the horizontal loads were applied to the tops

of the columns by a testing machine, having 30 tons capacity.

Side deflection was measured by a dial gauge at each horizontal load stage. A part of test results (load-deflection curves) have been plotted in Figs. 20, 21, 22, 23.

The dotted lines show the results calculated by Vogel's method. It is observed from Figs. 21~23,

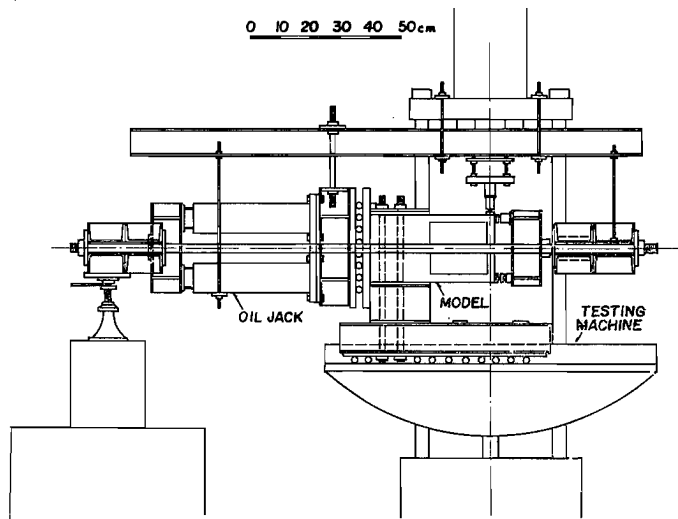


Fig. 20. Loading system.

that the horizontal maximum load considerably decreases as the axial force of columns increases. The horizontal load decreases once above the stability limit when $k=0.2$ or 0.4 and the amount of the deflection at the stability limit also decreases. When the axial force is large, the horizontal ultimate strength deviates largely from the values given by Vogel's method. The horizontal load becomes maximum when the frame has attained a mechanism, but when a column is subjected to a large axial force, the plastic zone extends along the longitudinal axis of the column above the elastic limit, so that the column stiffness is rapidly lost and the frame becomes unstable before the attainment of a mechanism.

The lower-storied columns of tall buildings are subjected to large axial forces so that the greatest care should be taken in the design of tall buildings.

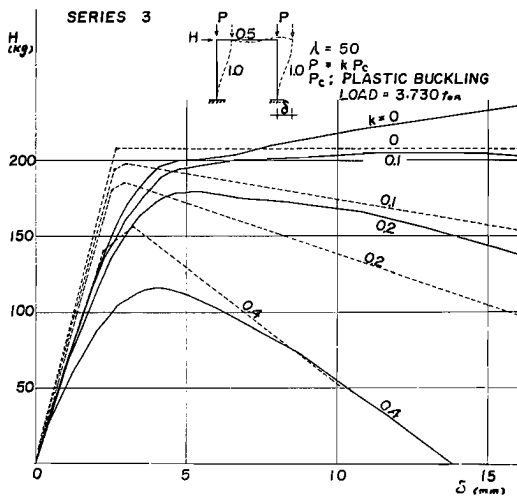


Fig. 21. Load-deflection curve.

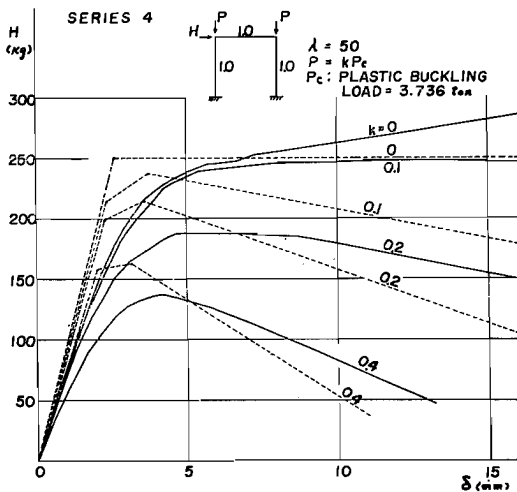


Fig. 22. Load-deflection curve.

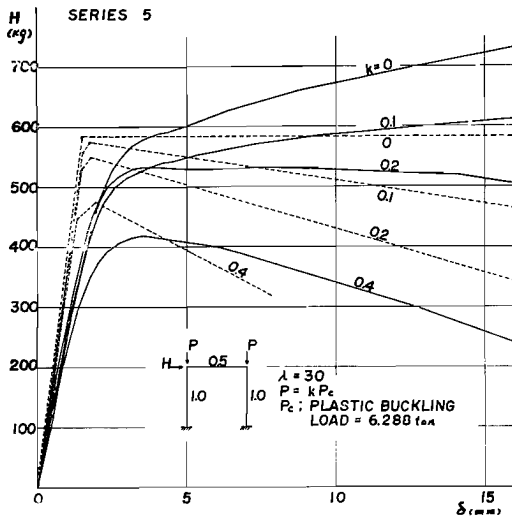


Fig. 23. Load-deflection curve.

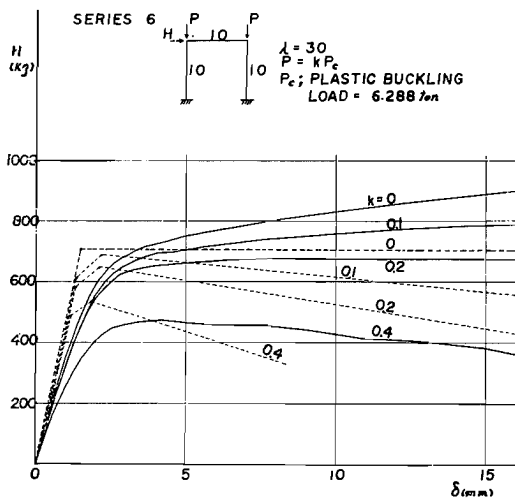


Fig. 24. Load-deflection curve.

4. Elasto-plastic behavior of frames and frames with diagonal bracing under repeated horizontal loading

4.1. A general survey of recent researches.

The structural strength, stiffness and damping are very important factors in the survival of structures under strong motion earthquakes. The structural stiffness is related to the fundamental period of vibration under dynamic loading. The earthquake feeds energy into a structure, and for survival the structure must consume all the energy imparted to it. The structural damping depends on many factors.

In the case of steel frames the damping depends mainly on the energy dissipation caused by the internal friction between structural elements and by the

inelastic deformation. To indicate the structural damping capacity quantitatively, it is required to perform many experiments under various structural conditions.

In our country, some experiments on various structures and structural elements have been carried out. In the case of steel structures, Tanabashi carried out experiments on riveted joints and welded joints, and showed that the riveted joints dissipate quite a lot of energy even under a small deflection^{10), 11)}.

Taniguchi conducted experiments on steel frames and joints, and showed that in steel structures the damping mainly depends on the internal friction between structural elements and on the inelastic deformation¹²⁾. Experiments on welded joints, riveted joints and bolted joints were carried out by Sumita and Igarashi, resulting in the discovery of the relationship between ductility factors and equivalent viscous damping capacities¹³⁾.

Onitake carried out experiments on braced frames and showed that the lowering of the structural stiffness is very small under repeated loading conditions even when the compression bracing buckles, and that the strength of structures does not change unfavourably even under buckling deformation of the compression bracing¹⁴⁾.

4.2. Some model tests of portal frames.

The author has conducted some experiments to find the general behaviour of steel structural frames under horizontal loading. Test frames are shown in Fig. 25. Four kinds of frames with rectangular cross sections have been tested under monotonous and repeated loading conditions. Their stiffness, restoring force and structural damping are discussed here. Test frames are made of the plate with 12 mm thickness only with the aid of machines, so that the residual stress by heat may be very small. Loading systems are also shown in Fig. 25. Horizontal deflections are measured by dial gauges and strain distributions by wire strain gauges.

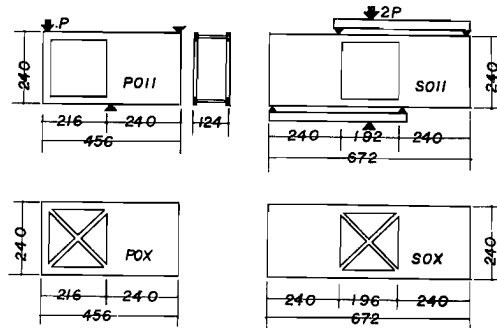


Fig. 25. Test frames and the loading system.

Monotonous loading conditions:

Under monotonous loading conditions, frames without bracing continue to deform in proportion to the increase of a load, and even after four plastic hinges are formed, the strength of frames increases by the strain hardening effect. Braced frames have a very high initial stiffness, but after the bracing yield, the stiffness is much abated. As the buckling deformation of the compression bracing increases, the axial force of compression bracing decreases, so that the frames with bracing attain their maximum load with a ductility factor of $\mu=5\sim 8$. Table 2 shows the comparison of the absorbed energy bet-

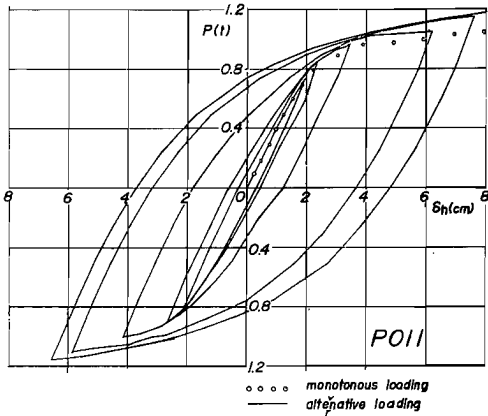


Fig. 26. (a) Load-deflection curve.

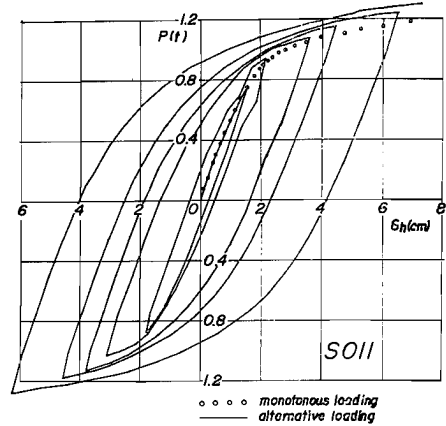


Fig. 26. (b) Load-deflection curve.

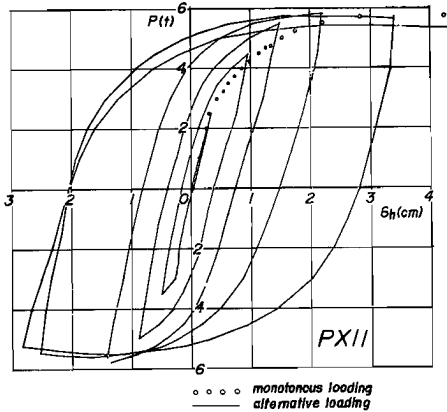


Fig. 26. (c) Load-deflection curve.

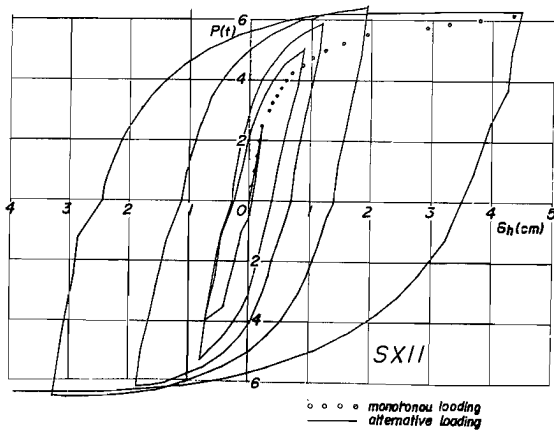


Fig. 26. (d) Load-deflection curve.

ween the experiment and the theory. As the initial stiffness of experimented frames is lower than the calculated, though their strength is higher than the calculated by 20%, their energy absorption is smaller under even fairly large deflection.

Repeated loading conditions:

Fig. 26 shows that under few repeated loadings Baushinger's effect is negligible in the case of frames without bracing, and that the lowering of stiffness is very small, even the buckling deformation of compression bracing occurs in the case of braced frames.

Fig. 27 shows the relations between deflections or ductility factors and specific damping capacities.

The frames without bracing absorb the energy mainly in the plastic deformations of plastic hinges, and braced frames absorb it mainly in the plastic deformation of bracings and plastic hinges. In the case of braced frames, the energy absorption is rather large even under small deflections. Equivalent viscous damping coefficient ratio

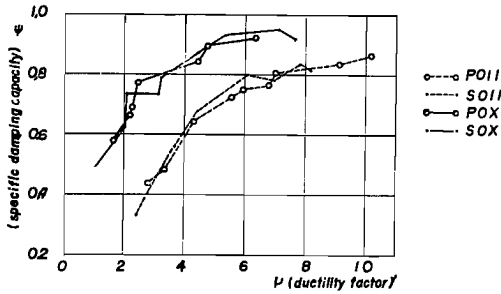


Fig. 27. (a) Specific damping capacity.

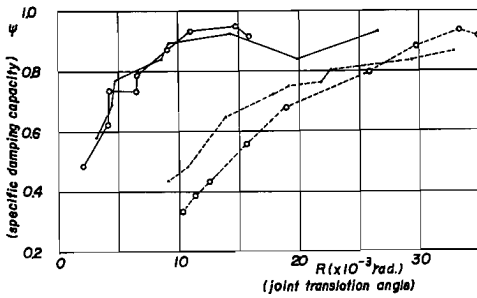


Fig. 27. (b) Specific damping capacity.

TABLE 2.
Comparison of absorbed energy.

	W _{exp.} /W _{cal.}			
R(rad.)	3 × 10 ⁻³	6 × 10 ⁻³	10 × 10 ⁻³	15 × 10 ⁻³
POII	0.74	0.72	0.80	0.85
SOII	0.67	0.63	0.76	0.88
PXII	0.75	0.82	0.92	0.93
SXII	0.83	0.88	0.95	1.00

$$W = \int_0^{R_h} PhdR \quad h : \text{height of frame}$$

$$R : \text{slope angle of column}$$

TABLE 3.
Equivalent viscous-damping coefficient ratio.

μ	2.0	3.0	5.0	8.0
POII	0.03	0.05	0.11	0.15
SOII	0.05	0.05	0.10	0.14
PXII	0.09	0.12	0.20	0.23
SXII	0.10	0.14	0.19	0.20

μ : ductility factor $\frac{\Delta\delta}{2\delta_y}$
 $\Delta\delta$: amplitude of deflection
 δ_y : calculated deflection at yield point

of portal frames, represented by a mechanical system —consisting of a single concentrated mass, a linear spring and viscous damping element having a damping force proportional to the relative velocity— is calculated and shown in Table 3.

5. Conclusions

In connection with the restoring force characteristics, which is the basis of the aseismic design of multi-story frames, the relation between the vertical force and the restoring characteristics, and the behaviour of frames under repeated horizontal loading are investigated. The influence of the vertical load on the restoring force characteristics is clarified in the elastic region and the design formula is proposed. In the elasto-plastic region, experimental results of miniature portal frames show that the theories are approximately substantiated by experimental results. The experiments on frames under repeated horizontal loading show that the frames with diagonal bracing have large energy absorption capacities and large ductility factors. The increase in the energy feeded from the ground into the frame with the increase of stiffness is supplemented by these effects. The adequately arranged bracing in multi-story frames is very effective as the aseismic structural element. The frames used for the experiment here are very small. In order to obtain more reliable data, it is necessary to experiment with larger frames like existing ones.

References

- (1) Muto, M. ; "Seismic Analysis of Reinforced Concrete Buildings", Proc. the World Conference on Earthquake Engineering, 34-1, (1956).
- (2) Wakabayashi, M. ; "On the Buckling of Uniform Multi-bay Frames", Report of A.I.J., No. 4 (Nov. 1949). (in Japanese)
- (3) Wakabayashi, M. ; "On the Buckling of Tall Frames with Varying Stiffness Ratio of Members", Report of A.I.J., No. 13 (Aug. 1951). (in Japanese)
- (4) Narita, H. ; "Project of Tokyo Station in 24 Storeys", Column, No. 3, p. 31, (June, 1962). (in Japanese)
- (5) Wakabayashi, M. ; "An Approximate Method of Buckling Analysis of Rectangular Frames", Report of A.I.J., No. 28 (II) (Nov. 1954). (in Japanese)
- (6) Kato, B. ; "Behavior of Short Columns Subjected to Lateral Force under High Compressive Stress", Trans. of A.I.J., No. 91 (Oct. 1963). (in Japanese) p. 15~p. 18.
- (7) Makino, M. ; "On the Study of Rectangular Struts Subjected to Axial Force and Bending Moment in Elasto-plastic Range", Trans. of A. I. J., No. 93 (Dec. 1963). p. 9~p. 13. (in Japanese)
- (8) Oxfort, J. ; "Über die Begrenzung der Traglast eines Statisch Unbestimmten Biegesteifen Stabwerkes aus Baustahl durch das Instabilwerden des Gleichgewichtes", Der Stahlbau, 30, H. 2, S. 33/46 (1961).
- (9) Vogel, U. ; "Über die Traglast Biegesteifer Stahlstabwerke", Der Stahlbau, 32, H. 4, S. 106/113 (1963).
- (10) Tanabashi, R. ; "Tests to Determine the Behavior of Riveted Joints of Steel Structures under Alternate Bending Moments", Memoirs of C.E.K. Kyoto Imp. Univ., vol. VIII, No. 4 (1935).
- (11) Tanabashi, R. ; "Tests to Determine the Behavior of Welded Joints of Steel Structures under Alternate Bending Moments", Jour. of J.W.S., vol. 9, No. 12 (1939).

- pp. 587-pp. 598. (in Japanese)
- (12) Taniguchi, T. ; "Analytical Investigation of Damping Factors of Various Building Constructions", Trans. of A.I.J., No. 17 (1940). pp. 339-pp. 346. (in Japanese)
 - (13) Sumita, S., Igarashi, S. and Tomoda, M. ; "Experimental Research for Plastic Connections of Steel Skeltons under Alternate Moment", of A.I.J., No. 69 (1961). pp. 114. (in Japanese)
 - (14) Onitake, N., Ando, M. and Kurino, T. ; "An Experimental study on Frames with Double Bracing of Light Gauge Steel", Trans. of A.I.J. No. 89 (1963). pp. 113. (in Japanese)